Horner-Wadsworth-Emmons Olefination of Proteins and Glycoproteins

Antonio Angelastro[1], Alexey Barkhanskiy[1], William R. F. Goundry[2], Perdita Barran[1], and Sabine L. Flitsch [1,]*

[1] Manchester Institute of Biotechnology (MIB) & School of Chemistry, The University of Manchester, 131 Princess Street, Manchester, M1 7DN, United Kingdom.

[2] The Department of Pharmaceutical Sciences, AstraZeneca, Silk Road Business Park, Macclesfield, Cheshire SK10 2NA, United Kingdom

* Corresponding Author E-mail: sabine.flitsch@manchester.ac.uk

ABSTRACT

Chemo-selective and site-specific modifications of proteins are fundamental to the advancement of biological and pharmaceutical sciences, from understanding the basis of cellular biology to development of biotherapeutics. Recent successes in bioconjugation chemistry have inspired the search for more biocompatible chemical reactions, which has prompted us to investigate Horner-Wadsworth-Emmons (HWE) olefinations, iconic reactions used widely in organic synthesis that would give rise to new selective protein olefinations. Our choice of HWE olefinations was inspired by the growing number of methods for the generation of aldehydes as transient reactive groups in proteins and the potential for mild and simple reaction conditions. Here we show that HWE on aldehydes produced by both chemical and enzymatic methods is fully compatible with physiological conditions and highly selective in small and large proteins, including therapeutic antibodies. By exploiting the wide range of easily accessible HWE reagents provided by organic chemistry, we show that the reaction kinetics can be fine-tuned over orders of magnitude by judicious use of substituents. The electrophilic nature of the HWE products can be tuned to allow for subsequent nucleophilic additions, including thiol- and phospha-Michael additions, enabling two-step dual labelling strategies. Our results demonstrate that HWE olefination of aldehydes in proteins provide efficient and selective bioconjugation chemistries that are orthogonal to existing methods.

INTRODUCTION

Bioconjugation chemistry has evolved from rudimental and stochastic modifications of a protein using carbodiimides and isothiocyanates to highly chemo-selective click chemistries,[1-3] notably Staudinger ligation,[4] [3+2] dipolar and Diels-Alder cycloadditions,[5-10] thiol-ene/yne,[11] aldol,[12,13] and transition-metal catalyzed reactions.[14] Hand in hand with the redeployment of traditional synthetic organic reactions to bioconjugation chemistry, the necessity to introduce bio-orthogonal moieties into proteins site-specifically also prompted the redevelopment of molecular biology and enzymology tools. The aldehyde moiety is a prominent example, as it is a functional group with versatile reactivity rarely found in proteins that can nevertheless be installed through a variety of chemical, enzymatic or genetic engineering techniques.[15] Likewise, a plethora of methodologies targeting the carbohydrate component of glycoproteins to introduce aldehyde tags are well-established.[15]

This ease of access to proteins and glycoproteins bearing aldehyde bio-orthogonal handles has made the development of technologies aimed at their further functionalization an increasingly researched topic in bioconjugation chemistry (Fig. 1). Classically, hydrazone and oxime ligation are perhaps the most popular methodologies for protein aldehyde conjugation,[16] but the susceptibility to hydrolysis of ligated end products triggered a quest for more robust chemistries, with particular attention on those forming C-C bonds. This has led to development of a series of conjugation technologies mainly based on Pictet-Spengler,[17-20] Knoevenagel,[21,22] aldol reactions,[13] and strain-promoted alkyne-nitrone cycloaddition (SPANC) (Fig. 1).[23] Given its prominence in organic chemistry, it is not surprising that Wittig olefination has been explored for protein functionalization[24] with some applications described for cell labelling[25,26] and phage libraries display. [27,28] However, harsh reaction conditions of Wittig olefination have failed to demonstrate use beyond the limited proof-of-concept stage.[29] In organic chemistry, a well-known alternative to Wittig reactions is the related Horner-Wadsworth-Emmons (HWE) olefination (Fig. 1), using a phosphonate-stabilized carbanion,[30,31] which can be used in aqueous conditions.[32] As a bio-orthogonal reaction, HWE is attractive for several reasons: (i) it does not require any additional reagents to the phosphonates, which are widely accessible, both commercially and synthetically, and well described in the literature; (ii) the resulting phosphate byproducts should be benign and easily removable; (iii) olefination introduces a small linker that should be stable under physiological conditions; (iv) finally, with judicious choice of substituents, the product could act

as an electrophile for secondary later stage modifications with additional nucleophiles, a unique aspect of HWE products compared to other conjugation strategies.

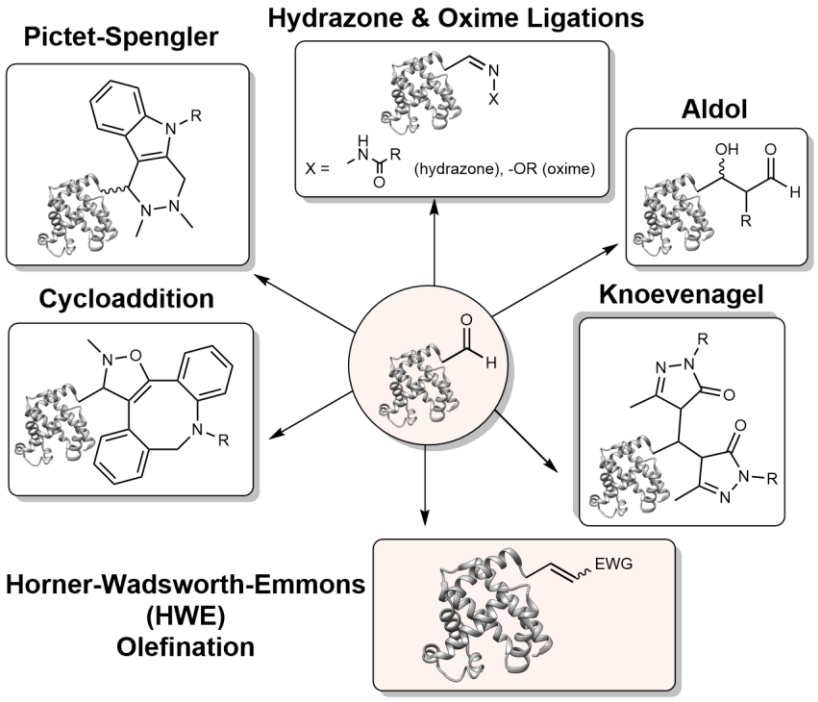

Fig. 1. Site-specific, bio-orthogonal functionalization of proteins through aldehydes. Protein aldehydes can be generated through enzymatic and chemical methods. The Horner-Wadsworth-Emmons (HWE) olefination is presented as a chemo-selective and biocompatible reaction generating a small stable linker (EWG = electron withdrawing group).

RESULTS

Exploring HWE chemistry on oxo-Myoglobin as a model protein aldehyde

Initial proof-of-concept studies were performed on oxo-Myoglobin **2**, which can be easily produced from **1** *via* oxidation with pyridoxal phosphate (Fig. 2a).[13] Upon reaction with a HWE reagent such as cyanophosphonate **a**, the corresponding protein acrylonitrile **3** was formed in >90% conversion after 2 h, as monitored by mass spectrometry (Fig. 2b). Encouraged by these results, a panel of phosphonates (**b-f**) was tested with similar success. Measurement of the time course of the reactions showed a spectrum of reactivity depending on the stabilizing substituent:

ketophosphonate **b** was ~3 fold less reactive than cyanophosphonate **a**, and conversion rates were noticeably slower for α-ester **c** and α-sulfone **d** substituted phosphonates. (Fig. 2a and Extended Data Fig 1). These kinetic data highlight the significant influence of the electron withdrawing group on the HWE reaction and provide a handle to tune reactivity of the reaction. Based on these data, it would be expected that difluorination increased reaction rate, which was indeed the case. Difluoro-substituted ketophosphonate **f,** resulted in ~8 times rate enhancement compared to its unsubstituted counterpart **e** (Fig. 2b).

The scope of the bioconjugation reaction to **2** was explored with phosphonates **a-i** leading to mg quantities of olefinated myoglobins **3-11** respectively. (For further examples see extended Data Fig. 2). Fluorinated phosphonate **f** proved to be the most efficient, with full conversion of **2** to **8** in less than 2 h in the presence of 10 mM **f** as shown by LC/MS analysis (Supplementary Information). The fluorine substituents in **8** allowed for direct detection using proton decoupled ^{19}F-NMR, with the diagnostic α,α-difluorovinylketone group visible as an AB quartet system at -114.2 and -115.8 ppm with a $^{2}J_{FF}$ of 144 Hz (Fig. 2b).

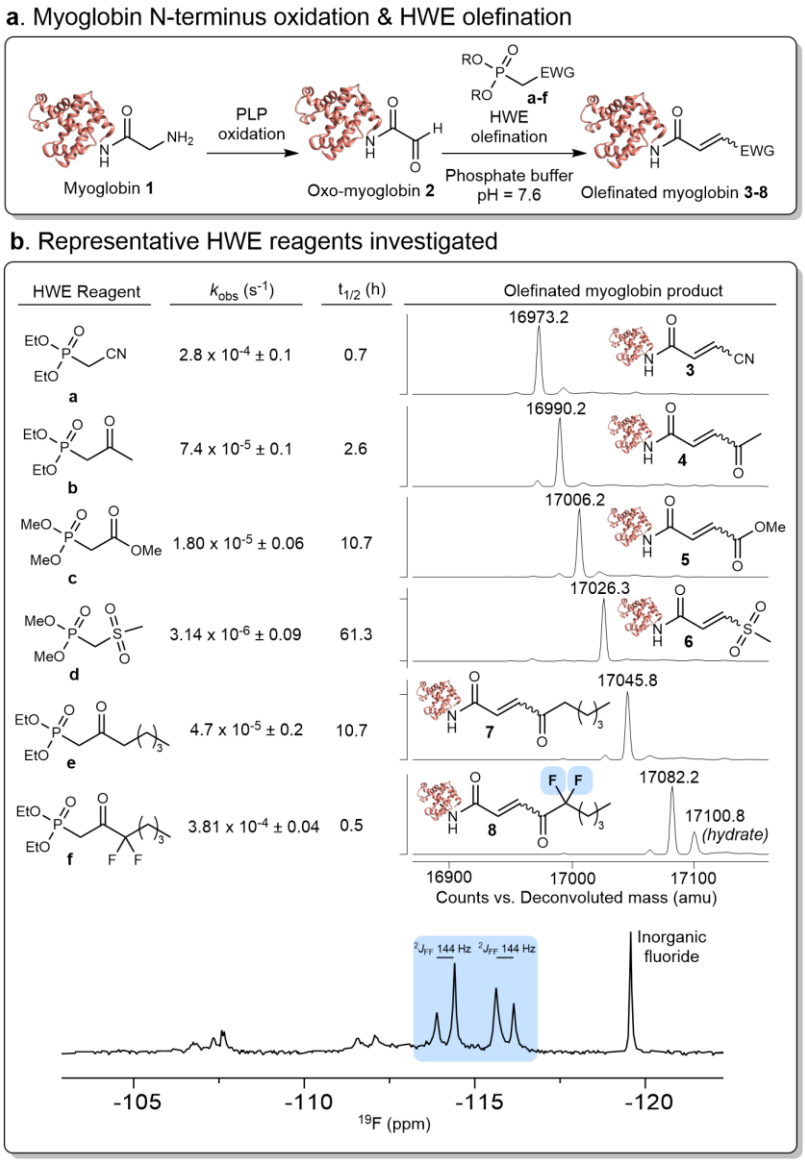

Fig. 2. **Horner-Wadsworth-Emmons (HWE) olefination of oxo-myoglobin 2**. (a) **2** was generated through oxidation of myoglobin **1** with pyridoxal phosphate (PLP) following established procedures and reacted with phosphonates **a-f**.[33] (b) Products of HWE reactions of phosphonates **a-f** with **2** were characterized by LC/MS and rates of reactions determined under pseudo-first order conditions (see Extended Data Fig. 1 and Supplementary Information for more details). Reactions for kinetic characterization were performed in 100 mM phosphate pH 7.6, 20 μM **2**, 50 mM **a-d**, while phosphonates **e-f** concentration was 10 mM. Proton decoupled ^{19}F-NMR of **8** was acquired in 10% D_2O 10 mM HEPES buffer pH 7.6. Minor ^{19}F peaks shifting downfield to the AB quartet are likely a manifestation of the equilibrium existing between the α,α-difluorovinylketone moiety and its hydrate form. Errors are intended as s.d. of the mean value. See Methods and Supplementary Information for more details.

Further functionalization of HWE olefination products

The electrophilicity of the HWE products **3-5** was further explored as a strategy for late-stage functionalization and potential for dual labelling (Fig. 3 and Extended Data Fig. 3-6). The reactivities of thiol- as well as phospha-Michael additions were monitored by LC/MS (Fig 3a), showing conversions to **16-27** consistent with the expected thiol- or phospha-Michael addition reactions (Fig. 3a and Extended Data Fig. 3). Unexpectedly, for myoglobin vinylsulfones **6** and **9** we observed desulfonylation as well as addition products (Fig. 3b and Extended Data Fig. 4-5), with desulfonation product **29** almost exclusively favoured over **30,** when protein vinylsulfone **6** was conjugated to the cationic cell-penetrating peptide Cys-TAT$_{(47\text{-}57)}$ **28** (Fig. 3b and Extended Data Fig. 5). Similarly, while reactivity of protein olefins **3-5** toward phosphine was consistent with a phospha-Michael addition, protein vinylsulfones **6** and **9** yielded exclusively desulfonylation products with no observable phospha-Michael adducts (Extended Data Fig. 4). Some further investigation into this surprising reaction outcome on small molecule equivalents such as *(E)*-3-(phenylsulfonyl)acrylamide, showed the same chemical behavior as its corresponding protein vinylsulfone **9** (Extended Data Fig. 6), suggesting that the desulfonation is not protein dependent.

These data show that the HWE reactions can install biorthogonal electrophiles into proteins (such as in **3-9)** as a strategy that is complementary to previous reports,[34] as it allows conjugation *via* phospha-Michael addition without resorting to metabolic engineering. The formation of protein-thiol **16** allows for even further conjugation *via* maleimide chemistry on a native protein lacking cysteine residues without employing mutagenesis (Fig. 3c).

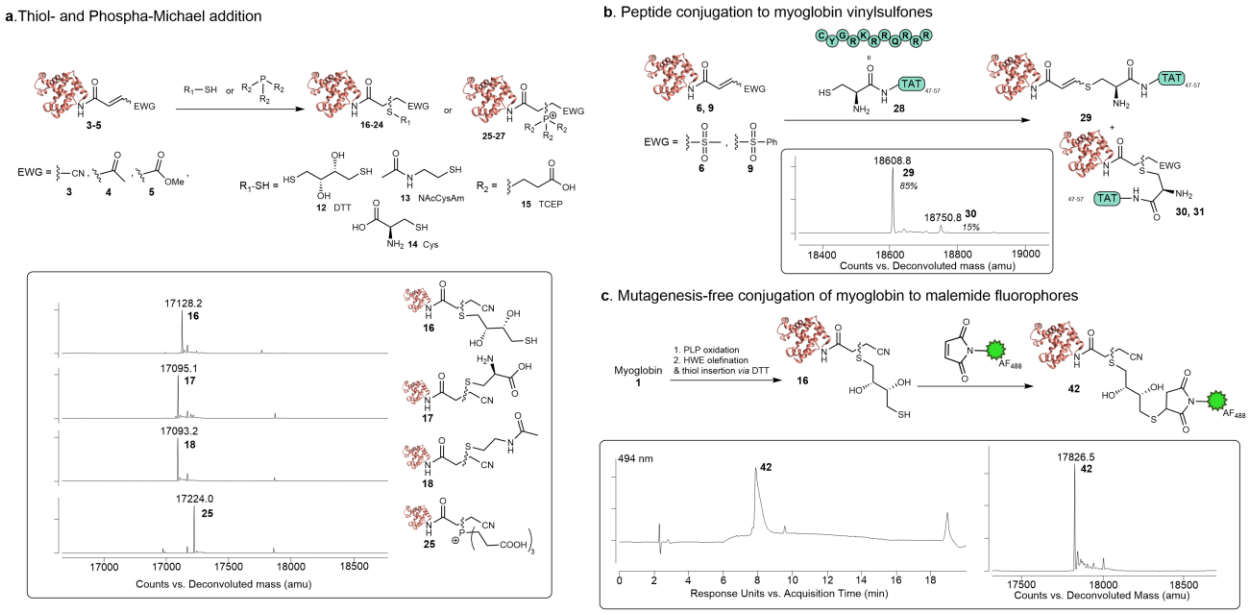

Fig. 3. **Late-stage functionalization reactions on olefinated myoglobins.** (a) Reactivity of olefinated myoglobins **3-5** towards thiols **12-14** and phosphine **15** leading to site-specific functionalization *via* either thiol- or phospha-Michael addition as demonstrated by LC/MS. (b) Myoglobin vinylsulfones **6** and **9** were conjugated to the cell-penetrating peptide Cys-TAT$_{47\text{-}57}$ **28** forming adducts **29** and **30**/**31**, respectively. (c) Further maleimide conjugation to **16.** See Extended Data Figs. 3-6 and Supplementary Information for further details.

Antibody olefination *via* glycoengineering

The issue of site-specific protein modification is particularly important for monoclonal antibodies (mAbs) - arguably the most complex glycoproteins of biopharmaceutical interest - and the production of their corresponding antibody-drug conjugates (ADCs). Glycoengineering methodologies are particularly attractive in this sense, as ADCs can be manufactured from the corresponding native mAb by targeting the N-glycan chain using glycoenzymes.[35-52] Many of the current conjugation technologies require the synthesis of complex nucleotide sugars or oligosaccharide building blocks modified with the desired biorthogonal functionality,[53] thus curtailing potential applications mainly to laboratory research.[47] Strategies using oxidative enzymes, such as Galactose oxidase (GOase), are more amenable to scale-up, as they generate biorthogonal aldehyde handles on the native mAb *in situ* by oxidizing naturally-occurring galactose units exposed on the non-reducing end of the N-glycan chain. The oxidized

galactoaldehyde can in turn be subjected to further functionalization using established conjugation chemistries such as tandem-Knoevenagel Michael-addition reaction, as previously shown by our group.[54]

With this premise, native antibody olefination represents the perfect benchmark to assess HWE chemistry in a much more challenging and clinically important context than oxidized myoglobin **2**. Trastuzumab is currently in the clinic for HER2 receptor positive breast and stomach cancers. The starting point for the present bioconjugation strategy is the previously described G2F/G2F glycoform **48**.[55] Both aldehyde formation using GOase M_1 variant and subsequent HWE olefination with cyanophosphonate **a** was performed as a one pot reaction with no need to isolate the intermediate aldehyde (Fig. 4a). Extensive characterization of the resulting Trastuzumab acrylonitrile **49** showed that modification was efficient and selective for the N-glycan chain (Fig. 4b and Extended Data Fig. 7). Intact antibody analysis of **49** (Extended Data Fig. 7) showed that all galactoside residues undergo acrylation upon treatment with GOase in the presence of the HWE reagent. The glycans were cleaved from **49** using PNGase resulting in unmodified protein backbone, thus confirming that the HWE reaction was selective for the glycan sidechain (Fig. 4b).

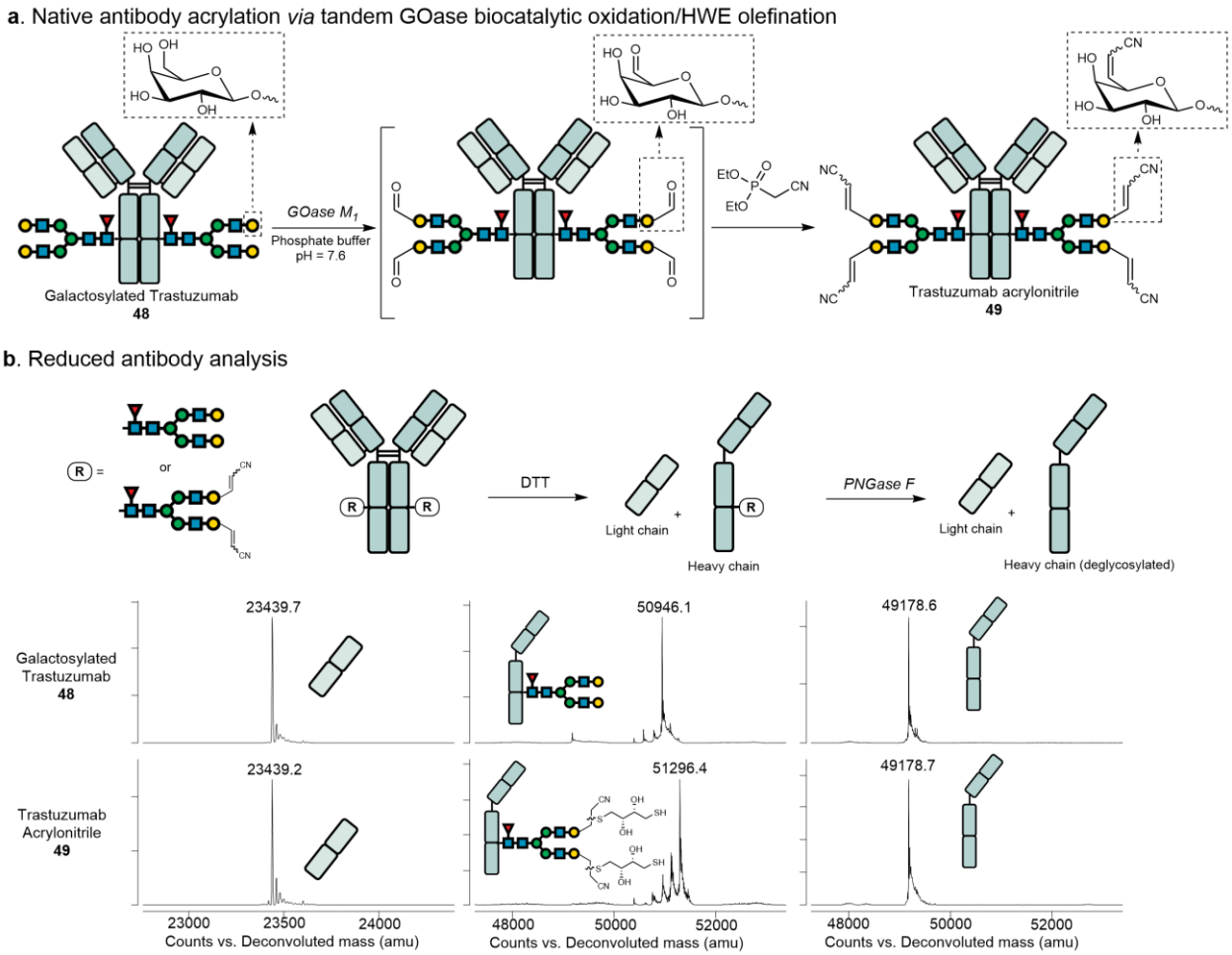

Fig. 4. **Glycoengineering of Trastuzumab *via* tandem enzymatic oxidation/Horner-Wadsworth-Emmons olefination**. (a) Trastuzumab **48** was converted to Trastuzumab acrylonitrile **49** by the combined action of the enzyme Galactose Oxidase and HWE with phosphonate **a**. (b) Antibody analysis of **48** and **49** after fragmentation show high selectivity to the antibody N-glycan chain and no modification of the protein backbone. See Extended Data Fig. 7 for further characterization of **49.**

CONCLUSIONS

In summary, we have shown Horner-Wadsworth-Emmons reaction can be employed as a versatile platform to generate olefinated proteins and glycoproteins selectively from their corresponding protein and glycoprotein aldehydes. The chemistry we have developed here allows us to install functional groups ranging from acrylonitrile to vinylsulfones, which can in turn be subjected to a wide range of late-stage functionalization reactions including thiol- and phospha-Michael addition. We show that HWE can be performed both on chemically generated protein

aldehydes such as oxo-myoglobin, as well as biocatalytically generated aldehydes, such as Trastuzumab. Given the broad range of strategies for introducing aldehydes into complex biomolecules through chemical, enzymatic and bioengineering approaches, the HWE olefination with its stable and easily accessible reagents and biocompatibility opens up a broad platform for enabling organic chemistry on complex molecules beyond proteins and glycoconjugates, including nucleic acids, lipids and biomaterials.

METHODS

Synthesis of olefinated myoglobins. Oxo-myoglobin **2** was produced following established procedures.[33] In a typical setup, 20 to 100 mg of myoglobin (0.7 mg/mL) from equine heart **1** was incubated with 25 mM pyridoxal phosphate (PLP) in 25 mM phosphate buffer pH 6.5 at 37 °C. Differently from the original protocol, incubation times where stretched from 18 to 36 h so to ensure full protein oxidation to aldehyde. After incubation, the resulting oxo-myoglobin was concentrated by ultrafiltration and buffer exchanged in 100 mM phosphate pH 7.6 using a Cytivia PD-10 desalting column. Oxo-myoglobin concentration was determined 7.3 mg/mL (428 μM) using an Eppendorf BioSpectrometer and extinction coefficient of 188000 M^{-1} cm^{-1} at 409 nm.[56] Subsequently, 5 mg of **2** (684μL, 7.3 mg/mL, 428 μM) in 100 mM phosphate buffer pH 7.6 was diluted to 5 mg/mL, added with the model HWE reagent and incubated at 25 °C using parameters as reported in Supplementary Data Table 1. Progress of each reaction was monitored by LC/MS (see Supplementary Methods) and excess of phosphonate was removed by buffer exchange in PBS pH = 7.4 using a Cytivia PD-10 desalting column when conversion was complete. Large scale production of fluorinated myoglobin **8** for NMR analysis was performed as described above using 40 mg of **2** and exchanging in 10% D_2O 10 mM HEPES pH = 7.6 using a PD-10 desalting column.

Extended Data Table 1. Paramenters used for production of olefinated myoglobins on large scale.

HWE reagent	Concentration (mM)	Incubation time
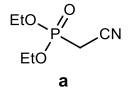 **a**	50	Overnight
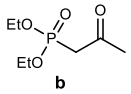 **b**	50	Overnight
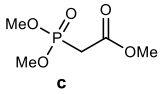 **c**	150	24 h
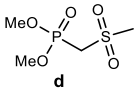 **d**	300	36 h
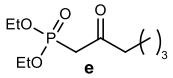 **e**	10	Overnight
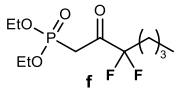 **f**	10	2 h
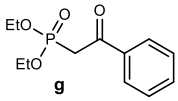 **g**	50	Overnight
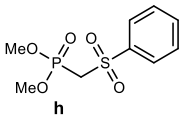 **h**	200 (10% DMSO)	36 h
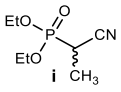 **i**	200	24 h

Kinetic analysis. Kinetic analysis for oxo-myglobin olefination was performed by recording a time-course of the reaction *via* UPLC/MS using a Waters Vion IMS QToF mass spectrometer equipped with a Acquity UPLC system and a Waters Acquity UPLC-BEH300 C4 (300 Å, 1.7 µm, 2.1 x 150 mm) column. Column temperature and flow were set at 45 °C and 0.2 mL/min, respectively. Injection volume for each time-point was 2 µL. After each injection, time-point samples were subjected to a linear gradient of 20% to 95% acetonitrile in 3 min (Supplementary Table 1). MS was set 2.00 kV capillary voltage, 120 °C source temperature, 400 °C desolvation acquired and raw data acquired in in positive mode between 500 and 2000 m/z with 0.250 s scan time. Autosampler temperature was set 25 °C. DAD acquisition was set on 215.0 and 280.0 nm.

In general, reactions were set up in a MS sample vial (50 – 100 µL final volume) where final concentration was of **2** was 20 µM while for model phosphonates **a-d** and **f-g** was 50 and 10 mM, respectively. The reaction was initiated by adding the phosphonate reagent as the last component immediately before the first LC/MS run (t = 0 h). Time courses of 1 h points were acquired by setting up in parallel two separate reactions in triplicate so that after the first run (t = 0 h) the next time point would be 1 h exactly. On the other hand, time points of 10 min each for formation of **3** and **8** had to be acquired in order to obtain a reliable k_{obs}. Because of a partial overlap of deconvoluted MS peaks between **2** and **3**, the kinetic course had to be acquired by derivatization of **3** product with addition of DTT in excess, which conferred a mass increase of +154 a.m.u. from the starting material thus allowing relative quantification (Supplementary figure 3).

Each raw MS time point was deconvoluted using MaxEnt function on Waters UNIFI software and exported to Origin Pro 2021b (Academic) SR9.8.5.212 for peak integration using the function "Peak Analyzer". Integrated peak areas associated to starting material and product were used to extrapolate starting material consumption through relative quantification. Pseudo-first order rate constants were determined by plotting ln[**2**] versus time and fitted to the following equation using Origin linear fit function: y = a + bx, where b represents the rate constant. Half-lives were determined with the following equation:

$$t_{1/2} = \frac{ln\,2}{k_{obs}} = \frac{0.693}{k_{obs}}$$

General setup for LC/MS analyses. Analyses were performed using either a Waters Vion IMS QToF mass spectrometer equipped with an Acquity UPLC system or an Agilent 6550 Ion Mobility LC/Q-TOF system equipped with a LC Agilent 1290 Infinity system. For reduced antibody analysis, an Agilent PLRP-S column (1000 Å, 5 μm, 2.1 x 50 mm) was used for LC separation while a Waters Acquity UPLC-BEH300 C4 (300 Å, 1.7 μm, 2.1 x 150 mm) column was employed for myoglobin and partially digested antibody analyses. Partial mAb digestion performed with IdeZ protease was carried out as previously described.[54]

Late-stage functionalization reactions on olefinated myoglobins. Probation of olefinated myoglobins reactivity toward model thiols **12-14** (10 mM) and phosphine **15** (1 mM) was performed in 100 mM phosphate pH = 8.0 by incubation the protein olefin (40 μM) with the model reagent for 4 h at room temperature before LC/MS analysis. Conjugation of myoglobin vinylsufones **6** and **9** to Cys-TAT_{47} **28** was performed using of the cell-penetrating peptide at 1 mM concentration.

Synthesis of Trastuzumab acrylonitrile from native Trastuzumab. Trastuzumab (30 mg, 6.9 mg/mL) in 100 mM Tris, 150 mM NaCl, (Tris-buffered saline, TBS), 5 mM $MnCl_2$, pH = 7.6 was incubated with *Hs*β4GalT1 (1 mg/mL) in presence of 15 mM UDP-Gal and at 37 °C for 20 h. After incubation, the resulting galactosylated antibody was purified by protein L affinity chromatography. Briefly, crude antibody was loaded on protein L agarose cartridge pre-equilibrated with TBS, and washed with 10 column volumes of TBS pH = 7.6. The antibody was eluted with 100 mM Gly buffer pH = 2.5; fractions containing the mAb were immediately neutralized with 1 M potassium phosphate dibasic to pH ≈ 7 and pooled together. The purified antibody was concentrated *via* ultrafiltration using a 30 kDa cutoff device and exchanged in 100 mM phosphate buffer pH 7.6 using a Cytvia PD-10 desalting column. Final yield was 25 mg. Subsequently, Galactosylated Trastuzumab (20 mg, 3.2 mg/mL) was incubated for 30 h at 37 °C with freshly prepared GOase-M_1 (2 mg/mL) in presence of Horseradish Peroxidase (HRP, 0.3 U/mL) and Catalase (50 U/mL) in 100 mM sodium phosphate buffer, 100 mM β-cyanophosphonate **a** pH = 7.6. Progress of GOase/HWE reaction was monitored by LC/MS by digesting for each time point 50 μg of mAb immobilized on Protein L magnetic beads with IdeZ protease. Trastuzumab Acrylonitrile was purified by protein L affinity chromatography and exchanged in PBS buffer pH 7.4 as described above for galactosylated Trastuzumab.

Trastuzumab acrylonitrile reaction with thiols. 50 μg of Trastuzumab acrylonitrile in 100 mM phosphate pH 8 were incubated for 24 h with 20 mM of either N-acetyl cysteamine **13** or cysteine **14** for 24 h. After incubation, the antibody was immobilized on Protein L magnetic beads and its corresponding Fc/2 fragment released in solution for LC/MS analysis through digestion with IdeZ protease, as previously described.[54]

Intact antibody analysis. Intact antibody samples were buffer exchanged twice into aqueous 200 mM ammonium acetate (Fisher Scientific, Loughborough, UK) using Zeba microspin columns (Fisher Scientific, Loughborough, UK) and diluted to ~1 μM concentration. Resultant solutions were analysed on QExactive UHMR (Thermo Fisher Scientific, US) equipped with a nanoelectrospray ion source. Spray emitters were produced on a micropipette puller P-2000 (Sutter, US) from borosilicate glass (O. D. 1.2 mm, I. D. 0.69 mm, 10 cm) purchased from World Precision Instruments, US. Platinum wire (Goodfellow) was used to provide electrical contact with sample solution loaded into the emitter.

Potentials and gas pressures were carefully optimised to maximise the transmission and removal of salt adducts while maintaining the structures intact. To achieve this, resolution setting was reduced to 12500 to minimise noise introduced into the spectra from ions that have collided with background gas molecules while being detected in the Orbitrap; extended trapping in the HCD cell was done to provide collisional cooling and therefore focus ions better in the C-trap prior to injection into the Orbitrap. Automatic gain control setting of 1E6 ions was used with all samples to remove the effect of space charge on mass accuracy. Optimised parameters for analysis are specified in Extended Data Table 2. Data was processed in Xcalibur Qual Browser (Thermo Fisher Scientific, US) and OriginPro 2019b (OriginLab Corporation, US). Mass and charge deconvolution was performed in UniDec using 'High-resolution Native' preset with sample mass every 1 Da.

Extended Data Table 2. Parameters for intact antibody analysis

Spray Voltage (kV)	0.9 - 1.1
Capillary Temp (°C)	300
S-lens RF Level (V)	200
Resolution	12500
AGC Target (ions)	1E6
Maximum Inject Time (ms)	100
Detector m/z Settings	low m/z
Ion Transfer m/z Settings	low m/z
Source DC Offset (V)	21
In-Source CID (V)	20
Extended Trapping (V)	50V
HCD Gas Flow	2

DATA AVAILABILITY

The data supporting the findings are available within the article, its Supplementary Information or can be obtained from the corresponding author on reasonable request.

ACKNOWLEDGMENTS

The authors acknowledge funding by the EPSRC, BBSRC, and AstraZeneca plc under the Prosperity Partnership EP/S005226/1. The authors are grateful to Dr. Matthew Cliff and Reynard Speiss for their support with ^{19}F-NMR and MS analyses, respectively.

AUTHOR CONTRIBUTIONS

S.L.F., W.R.F.G., and P.B. managed and supervised the project. S.L.F., A.A., and W.R.F.G. devised the concept. A.A. performed myoglobin olefination experiments including their kinetic, LC/MS and ^{19}F-NMR analyses. A.A. performed large scale production of olefinated myoglobins. A.A. developed the one-pot GOase/HWE glycoengineering strategy, performed Trastuzumab acrylonitrile synthesis and MS analyses of reduced and partially digested antibodies. A.B.

performed intact antibody analysis. A.A., S.L.F. W.R.F.G., and A.B. wrote the manuscript and generated figures.

COMPETING INTERESTS STATEMENT

The authors declare no competing interests.

AUTHOR INFORMATION

Corresponding Author E-mail: sabine.flitsch@manchester.ac.uk

Notes

The authors declare no competing financial interests.

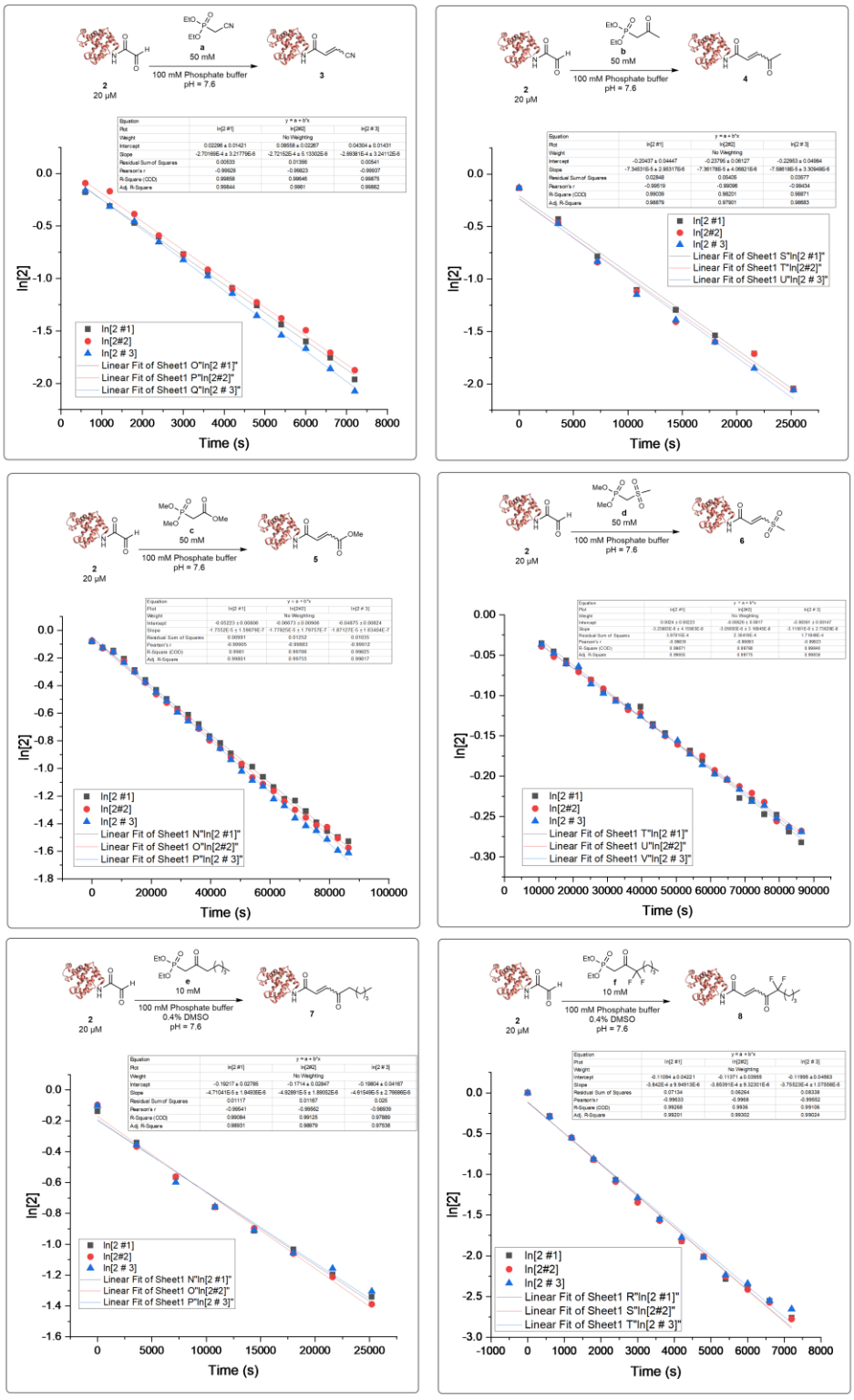

Extended Data Fig. 1. Kinetic analysis under pseudo-first order conditions of phosphonates **a-f** reactivity toward oxo-myoglobin **2**.

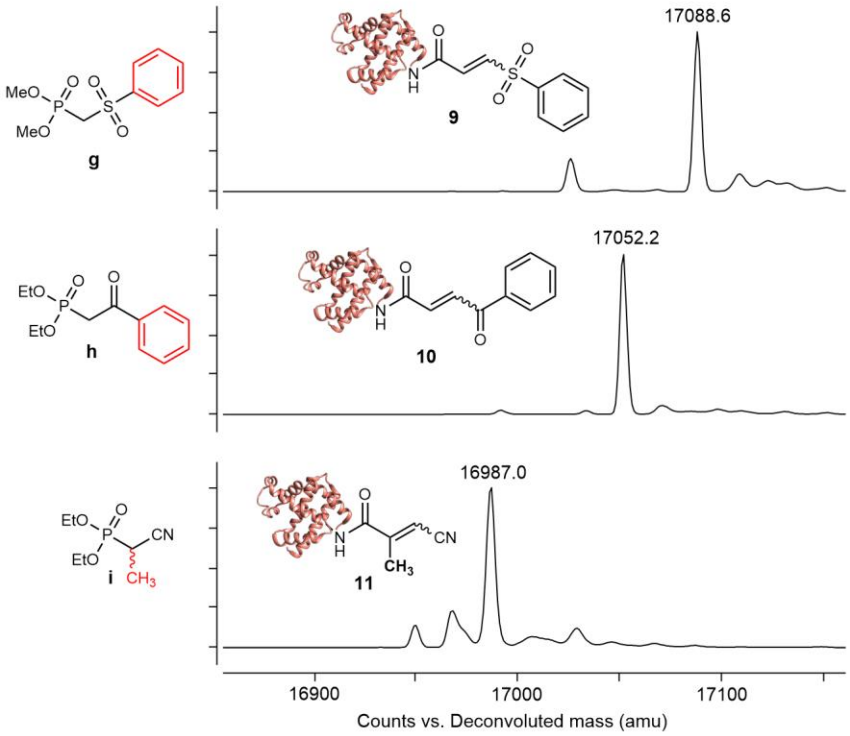

Extended Data Fig. 2. Reaction of oxo-Myoglobin **2** with substituted phosphonates derived from HWE reagents **a**, **b** and **d**.

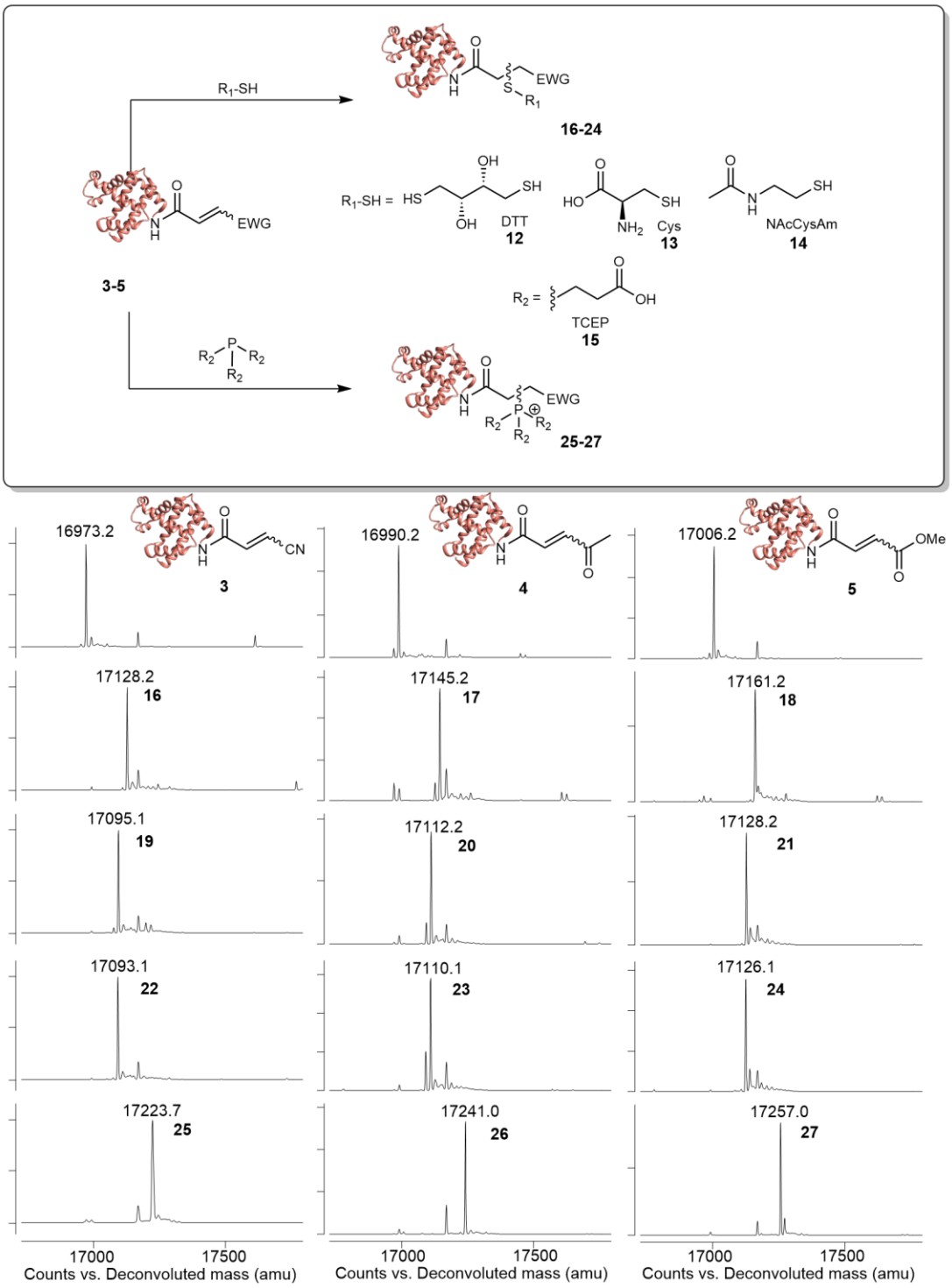

Extended Data Fig. 3. Reactivity of olefinated myoglobins **3-5** toward either thiol- or phosha-Michael addition using model thiols or phosphine, respectively.

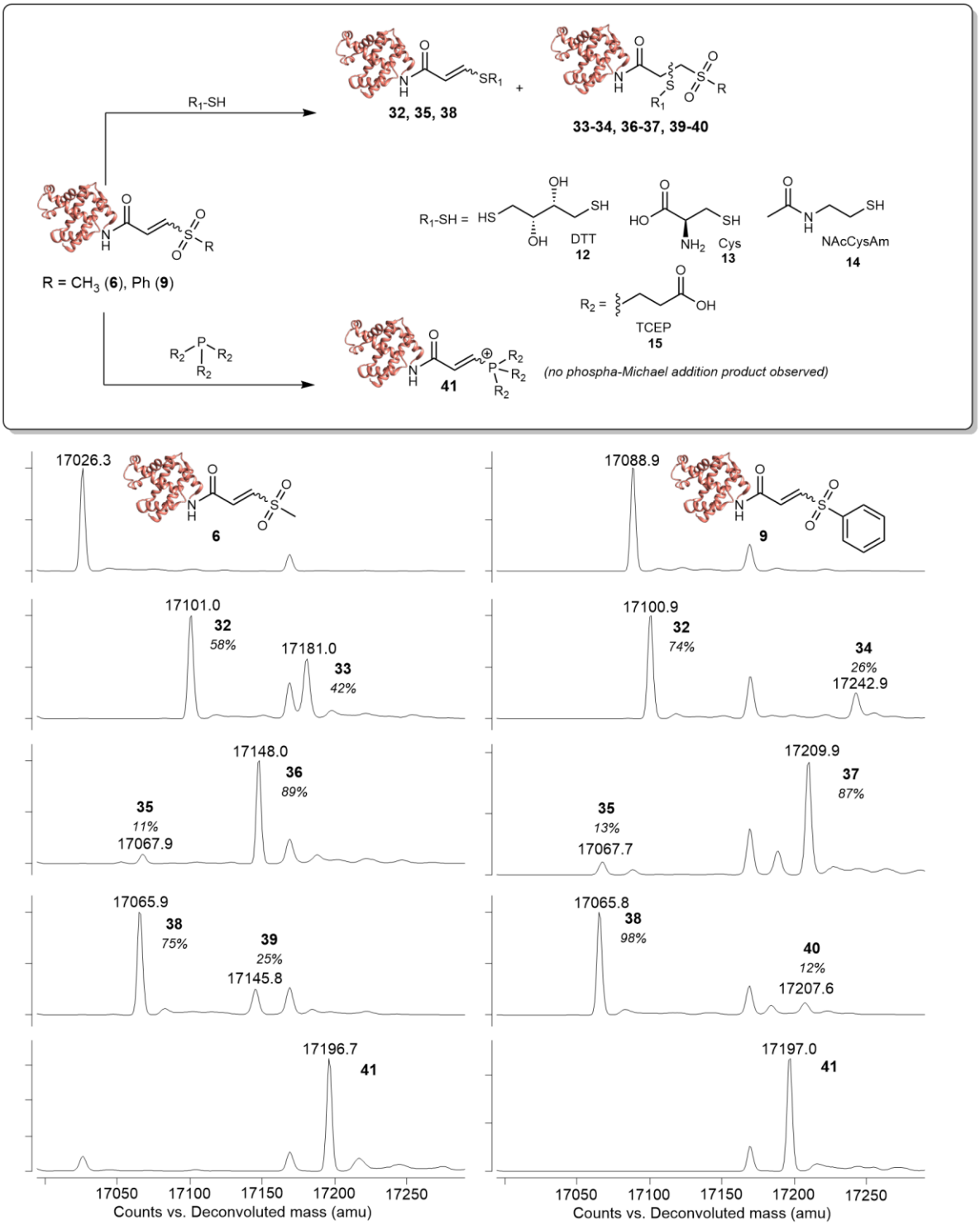

Extended Data Fig. 4. Reactivity of myoglobin vinylsulfones toward model thiols and phosphine. While thiols yield either thiol-Michael or desulfonylated products from **6** and **9** with different ratios, only the desulfonylated adduct **15** was observed upon reaction with phosphine.

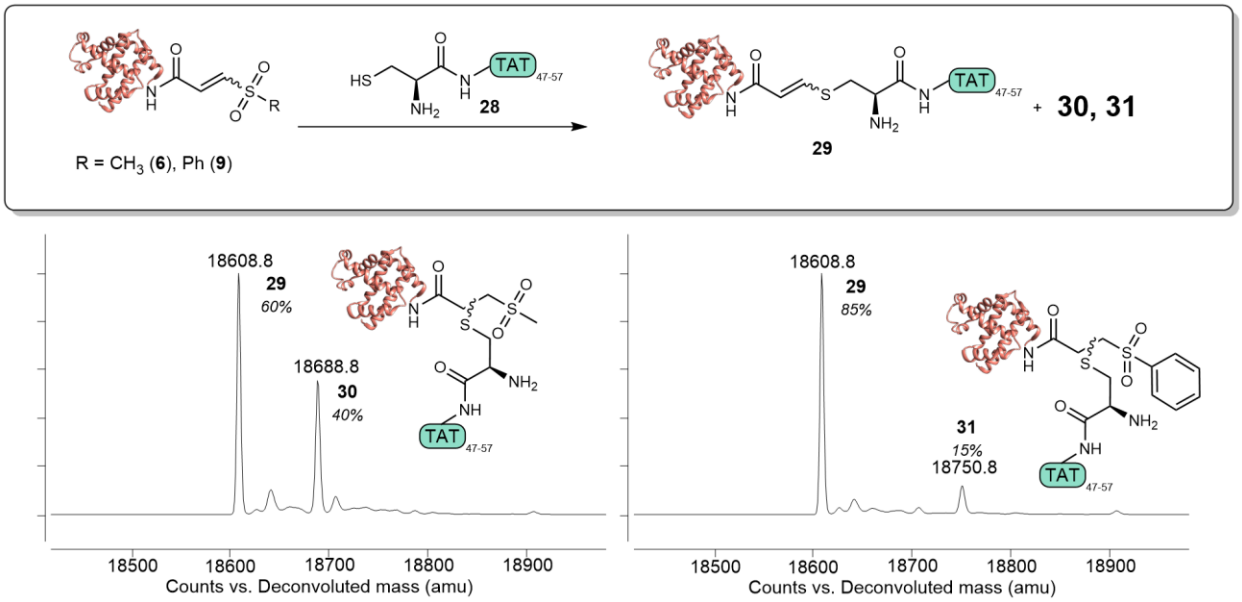

Extended Data Fig. 5. Comparisons between reactivity of myoglobin vinylsulfones **6** and **9** toward the cell-penetrating peptide **28**.

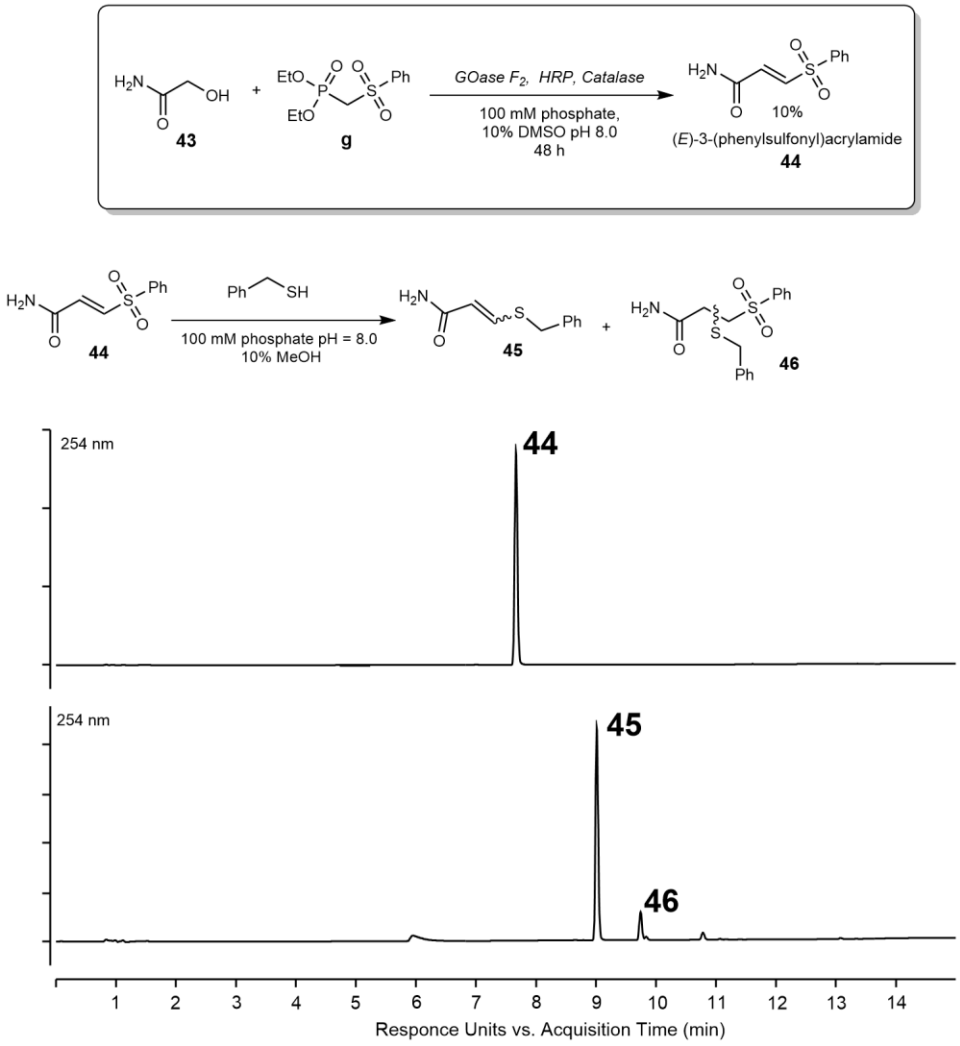

Extended Data Fig. 6. Chemoenzymatic synthesis and reactivity of *(E)*-3-(phenylsulfonyl)acrylamide toward benzylmercaptan. The model compound shows same reactivity as for myoglobin vinylsulfones. See supplementary information for further details.

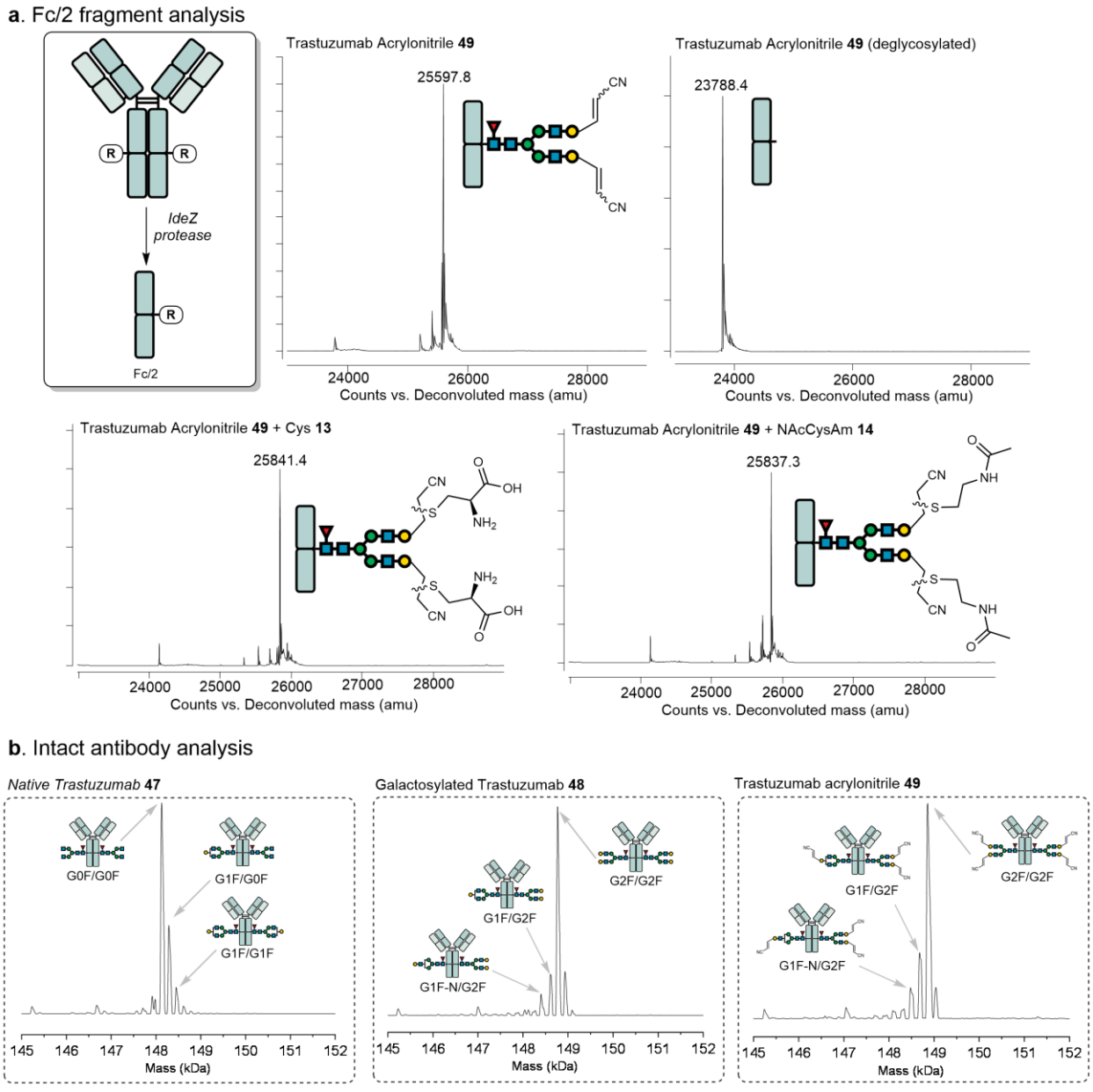

Extended Data Fig. 7. Characterization of acrylo-Trastuzumab **a.** reduced and **b.** partially digested antibdoby analysis.

REFERENCES

1 Bird, R. E., Lemmel, S. A., Yu, X. & Zhou, Q. A. Bioorthogonal Chemistry and Its Applications. *Bioconjug Chem* **32**, 2457-2479, doi:10.1021/acs.bioconjchem.1c00461 (2021).

2 Bertozzi, C. R. A decade of bioorthogonal chemistry. *Acc Chem Res* **44**, 651-653, doi:10.1021/ar200193f (2011).

3 Sornay, C., Vaur, V., Wagner, A. & Chaubet, G. An overview of chemo- and site-selectivity aspects in the chemical conjugation of proteins. *R Soc Open Sci* **9**, 211563, doi:10.1098/rsos.211563 (2022).

4 Bednarek, C., Wehl, I., Jung, N., Schepers, U. & Bräse, S. The Staudinger Ligation. *Chemical Reviews*, doi:10.1021/acs.chemrev.9b00665 (2020).

5 Meldal, M. & Tornoe, C. W. Cu-catalyzed azide-alkyne cycloaddition. *Chem Rev* **108**, 2952-3015, doi:10.1021/cr0783479 (2008).

6 Agard, N. J., Prescher, J. A. & Bertozzi, C. R. A Strain-Promoted [3 + 2] Azide−Alkyne Cycloaddition for Covalent Modification of Biomolecules in Living Systems. *Journal of the American Chemical Society* **126**, 15046-15047, doi:10.1021/ja044996f (2004).

7 Wang, Q. *et al.* Bioconjugation by copper(I)-catalyzed azide-alkyne [3 + 2] cycloaddition. *J Am Chem Soc* **125**, 3192-3193, doi:10.1021/ja021381e (2003).

8 McKay, C. S., Moran, J. & Pezacki, J. P. Nitrones as dipoles for rapid strain-promoted 1,3-dipolar cycloadditions with cyclooctynes. *Chem Commun (Camb)* **46**, 931-933, doi:10.1039/b921630h (2010).

9 St Amant, A. H. *et al.* A Diene-Containing Noncanonical Amino Acid Enables Dual Functionality in Proteins: Rapid Diels-Alder Reaction with Maleimide or Proximity-Based Dimerization. *Angew Chem Int Ed Engl* **58**, 8489-8493, doi:10.1002/anie.201903494 (2019).

10 Blackman, M. L., Royzen, M. & Fox, J. M. Tetrazine ligation: fast bioconjugation based on inverse-electron-demand Diels-Alder reactivity. *J Am Chem Soc* **130**, 13518-13519, doi:10.1021/ja8053805 (2008).

11 Stenzel, M. H. Bioconjugation Using Thiols: Old Chemistry Rediscovered to Connect Polymers with Nature's Building Blocks. *ACS Macro Lett* **2**, 14-18, doi:10.1021/mz3005814 (2013).

12 Keenan, T. *et al.* A Tale of Two Bioconjugations: pH Controlled Divergent Reactivity of Protein alpha-oxo-Aldehydes in Competing alpha-oxo-Mannich and Catalyst-Free Aldol Ligations. *ACS Chem Biol* **16**, 2387-2400, doi:10.1021/acschembio.1c00531 (2021).

13 Spears, R. J. *et al.* Site-selective C–C modification of proteins at neutral pH using organocatalyst-mediated cross aldol ligations. *Chemical Science* **9**, 5585-5593, doi:10.1039/c8sc01617h (2018).

14 Rodriguez, J. & Martinez-Calvo, M. Transition-Metal-Mediated Modification of Biomolecules. *Chemistry* **26**, 9792-9813, doi:10.1002/chem.202001287 (2020).

15 Spears, R. J. & Fascione, M. A. Site-selective incorporation and ligation of protein aldehydes. *Org Biomol Chem* **14**, 7622-7638, doi:10.1039/c6ob00778c (2016).

16 Rannes, J. B. *et al.* Glycoprotein labeling using engineered variants of galactose oxidase obtained by directed evolution. *J Am Chem Soc* **133**, 8436-8439, doi:10.1021/ja2018477 (2011).

17 Agarwal, P., van der Weijden, J., Sletten, E. M., Rabuka, D. & Bertozzi, C. R. A Pictet-Spengler ligation for protein chemical modification. *Proceedings of the National Academy of Sciences* **110**, 46-51, doi:10.1073/pnas.1213186110 (2012).

18 Agarwal, P. *et al.* Hydrazino-Pictet-Spengler Ligation as a Biocompatible Method for the Generation of Stable Protein Conjugates. *Bioconjugate Chem* **24**, 846-851, doi:10.1021/bc400042a (2013).

19 Drake, P. M. *et al.* Aldehyde tag coupled with HIPS chemistry enables the production of ADCs conjugated site-specifically to different antibody regions with distinct in vivo efficacy and PK outcomes. *Bioconjug Chem* **25**, 1331-1341, doi:10.1021/bc500189z (2014).

20 Pomplun, S., Mohamed, M. Y. H., Oelschlaegel, T., Wellner, C. & Bergmann, F. Efficient Pictet-Spengler Bioconjugation with N-Substituted Pyrrolyl Alanine Derivatives. *Angewandte Chemie International Edition* **58**, 3542-3547, doi:10.1002/anie.201814200 (2019).

21 Kudirka, R. *et al.* Generating Site-Specifically Modified Proteins via a Versatile and Stable Nucleophilic Carbon Ligation. *Chemistry & Biology* **22**, 293-298, doi:10.1016/j.chembiol.2014.11.019 (2015).

22 Yu, J., Shen, D., Zhang, H. & Yin, Z. Rapid, Stoichiometric, Site-Specific Modification of Aldehyde-Containing Proteins Using a Tandem Knoevenagel-Intra Michael Addition Reaction. *Bioconjug Chem* **29**, 1016-1020, doi:10.1021/acs.bioconjchem.8b00086 (2018).

23 Ning, X. *et al.* Protein Modification by Strain-Promoted Alkyne-Nitrone Cycloaddition. *Angewandte Chemie International Edition* **49**, 3065-3068, doi:10.1002/anie.201000408 (2010).

24 Han, M.-J., Xiong, D.-C. & Ye, X.-S. Enabling Wittig reaction on site-specific protein modification. *Chem Commun* **48**, doi:10.1039/c2cc35738k (2012).

25 Lum, K. M., Xavier, V. J., Ong, M. J. H., Johannes, C. W. & Chan, K.-P. Stabilized Wittig olefination for bioconjugation. *Chem Commun* **49**, doi:10.1039/c3cc45961f (2013).

26 McLeod, D. & McNulty, J. Mild Chemical and Biological Synthesis of Donor-Acceptor Flanked Reporter Stilbenes: Demonstration of a Physiological Wittig Olefination Reaction. *Eur J Org Chem* **2012**, 6127-6131, doi:10.1002/ejoc.201201042 (2012).

27 Triana, V. & Derda, R. Tandem Wittig/Diels–Alder diversification of genetically encoded peptide libraries. *Organic & Biomolecular Chemistry* **15**, 7869-7877, doi:10.1039/c7ob01635b (2017).

28 Yan, K. *et al.* Learning the structure-activity relationship (SAR) of the Wittig reaction from genetically-encoded substrates. *Chem Sci* **12**, 14301-14308, doi:10.1039/d1sc04146k (2021).

29 Dadová, J., Galan, S. R. G. & Davis, B. G. Synthesis of modified proteins via functionalization of dehydroalanine. *Current Opinion in Chemical Biology* **46**, 71-81, doi:10.1016/j.cbpa.2018.05.022 (2018).

30 Maryanoff, B. E. & Reitz, A. B. The Wittig olefination reaction and modifications involving phosphoryl-stabilized carbanions. Stereochemistry, mechanism, and selected synthetic aspects. *Chemical Reviews* **89**, 863-927, doi:10.1021/cr00094a007 (2002).

31 Beemelmanns, C., Roman, D. & Sauer, M. Applications of the Horner–Wadsworth–Emmons Olefination in Modern Natural Product Synthesis. *Synthesis* **53**, 2713-2739, doi:10.1055/a-1493-6331 (2021).

32 Gijsen, H. J. M. & Wong, C.-H. Synthesis of a cyclitol via a tandem enzymatic aldol — intramolecular Horner-Wadsworth-Emmons reaction. *Tetrahedron Lett* **36**, 7057-7060, doi:10.1016/0040-4039(95)01483-x (1995).

33 Spears, R. J. *et al.* Site-selective C-C modification of proteins at neutral pH using organocatalyst-mediated cross aldol ligations. *Chem Sci* **9**, 5585-5593, doi:10.1039/c8sc01617h (2018).

34 Lee, Y. J., Kurra, Y. & Liu, W. R. Phospha-Michael Addition as a New Click Reaction for Protein Functionalization. *Chembiochem* **17**, 456-461, doi:10.1002/cbic.201500697 (2016).

35 Wang, L. X., Tong, X., Li, C., Giddens, J. P. & Li, T. Z. Glycoengineering of Antibodies for Modulating Functions. *Annual Review of Biochemistry, Vol 88* **88**, 433-459, doi:10.1146/annurev-biochem-062917-012911 (2019).

36 Huang, W., Giddens, J., Fan, S. Q., Toonstra, C. & Wang, L. X. Chemoenzymatic glycoengineering of intact IgG antibodies for gain of functions. *J Am Chem Soc* **134**, 12308-12318, doi:10.1021/ja3051266 (2012).

37 Zuberbuhler, K., Casi, G., Bernardes, G. J. & Neri, D. Fucose-specific conjugation of hydrazide derivatives to a vascular-targeting monoclonal antibody in IgG format. *Chem Commun (Camb)* **48**, 7100-7102, doi:10.1039/c2cc32412a (2012).

38 Okeley, N. M. *et al.* Metabolic engineering of monoclonal antibody carbohydrates for antibody-drug conjugation. *Bioconjug Chem* **24**, 1650-1655, doi:10.1021/bc4002695 (2013).

39 Li, X., Fang, T. & Boons, G. J. Preparation of well-defined antibody-drug conjugates through glycan remodeling and strain-promoted azide-alkyne cycloadditions. *Angew Chem Int Ed Engl* **53**, 7179-7182, doi:10.1002/anie.201402606 (2014).

40 Zeglis, B. M. *et al.* Chemoenzymatic Strategy for the Synthesis of Site-Specifically Labeled Immunoconjugates for Multimodal PET and Optical Imaging. *Bioconjugate Chem* **25**, 2123-2128, doi:10.1021/bc500499h (2014).

41 Thompson, P. *et al.* Straightforward Glycoengineering Approach to Site-Specific Antibody–Pyrrolobenzodiazepine Conjugates. *ACS Medicinal Chemistry Letters* **7**, 1005-1008, doi:10.1021/acsmedchemlett.6b00278 (2016).

42 van Geel, R. *et al.* Chemoenzymatic Conjugation of Toxic Payloads to the Globally Conserved N-Glycan of Native mAbs Provides Homogeneous and Highly Efficacious Antibody-Drug Conjugates. *Bioconjug Chem* **26**, 2233-2242, doi:10.1021/acs.bioconjchem.5b00224 (2015).

43 Zhou, Q. *et al.* Site-specific antibody-drug conjugation through glycoengineering. *Bioconjug Chem* **25**, 510-520, doi:10.1021/bc400505q (2014).

44 Qasba, P. K. Glycans of Antibodies as a Specific Site for Drug Conjugation Using Glycosyltransferases. *Bioconjug Chem* **26**, 2170-2175, doi:10.1021/acs.bioconjchem.5b00173 (2015).

45 Mastrangeli, R., Palinsky, W. & Bierau, H. Glycoengineered antibodies: towards the next-generation of immunotherapeutics. *Glycobiology* **29**, 199-210, doi:10.1093/glycob/cwy092 (2019).

46 Li, T., Tong, X., Yang, Q., Giddens, J. P. & Wang, L. X. Glycosynthase Mutants of Endoglycosidase S2 Show Potent Transglycosylation Activity and Remarkably Relaxed Substrate Specificity for Antibody Glycosylation Remodeling. *J Biol Chem* **291**, 16508-16518, doi:10.1074/jbc.M116.738765 (2016).

47 Manabe, S. *et al.* Characterization of Antibody Products Obtained through Enzymatic and Nonenzymatic Glycosylation Reactions with a Glycan Oxazoline and Preparation of a Homogeneous Antibody-Drug Conjugate via Fc N-Glycan. *Bioconjug Chem* **30**, 1343-1355, doi:10.1021/acs.bioconjchem.9b00132 (2019).

48 Tang, F. *et al.* One-pot N-glycosylation remodeling of IgG with non-natural sialylglycopeptides enables glycosite-specific and dual-payload antibody–drug conjugates. *Organic & Biomolecular Chemistry* **14**, 9501-9518, doi:10.1039/c6ob01751g (2016).

49 Fairbanks, A. J. Chemoenzymatic synthesis of glycoproteins. *Curr Opin Chem Biol* **53**, 9-15, doi:10.1016/j.cbpa.2019.05.015 (2019).

50 Sjogren, J., Lood, R. & Nageli, A. On enzymatic remodeling of IgG glycosylation; unique tools with broad applications. *Glycobiology* **30**, 254-267, doi:10.1093/glycob/cwz085 (2020).

51 Boeggeman, E. *et al.* Site specific conjugation of fluoroprobes to the remodeled Fc N-glycans of monoclonal antibodies using mutant glycosyltransferases: application for cell surface antigen detection. *Bioconjug Chem* **20**, 1228-1236, doi:10.1021/bc900103p (2009).

52 Majewska, N. I., Tejada, M. L., Betenbaugh, M. J. & Agarwal, N. N-Glycosylation of IgG and IgG-Like Recombinant Therapeutic Proteins: Why Is It Important and How Can We Control It? *Annu Rev Chem Biomol Eng*, doi:10.1146/annurev-chembioeng-102419-010001 (2020).

53 Fairbanks, A. J. Synthetic and semi-synthetic approaches to unprotected N-glycan oxazolines. *Beilstein Journal of Organic Chemistry* **14**, 416-429, doi:10.3762/bjoc.14.30 (2018).

54 Angelastro, A. *et al.* Galactose Oxidase Enables Modular Assembly of Conjugates from Native Antibodies with High Drug-to-Antibody Ratios. *ChemSusChem* **15**, e202102592, doi:10.1002/cssc.202102592 (2022).

55 Upton, R. *et al.* Hybrid mass spectrometry methods reveal lot-to-lot differences and delineate the effects of glycosylation on the tertiary structure of Herceptin(R). *Chem Sci* **10**, 2811-2820, doi:10.1039/c8sc05029e (2019).

56 Bostelaar, T. *et al.* Hydrogen Sulfide Oxidation by Myoglobin. *J Am Chem Soc* **138**, 8476-8488, doi:10.1021/jacs.6b03456 (2016).